Solution Structure of Human Intestinal Fatty Acid Binding Protein with a Naturally-Occurring Single Amino Acid Substitution (A54T) that Is Associated with Altered Lipid Metabolism[†,‡]

Fengli Zhang,[§] Christian Lücke,[§,||,⊥] Leslie J. Baier,[@] James C. Sacchettini,[#] and James A. Hamilton*[,§]

Department of Physiology and Biophysics, Boston University School of Medicine, Boston, Massachusetts 02118, Institut für Biophysikalische Chemie, Johann Wolfgang Goethe-Universität, 60439 Frankfurt am Main, Germany, Phoenix Epidemiology and Clinical Research Branch, National Institute of Diabetes and Digestive and Kidney Diseases, National Institutes of Health, Phoenix, Arizona 85016, and Department of Biochemistry and Biophysics, Texas A&M University, College Station, Texas 77845

Received December 16, 2002; Revised Manuscript Received April 17, 2003

ABSTRACT: The human intestinal fatty acid binding protein (I-FABP) belongs to a family of intracellular lipid binding proteins. This 15 kDa protein binds dietary long-chain fatty acids in the cytosol of enterocytes. A naturally-occurring nucleotide polymorphism at codon 54, which produces either an alanine-containing (A54) or a threonine-containing (T54) protein, has been identified. These two I-FABP forms display differential binding and transport of fatty acids across cells, and their alleles are associated with *in vivo* insulin resistance and/or altered lipid metabolism in several human populations. The three-dimensional solution structure of the more common A54 form was previously determined in our lab. A direct comparison between human A54 and T54 I-FABP has now been performed to help elucidate the structural origins of their physiological distinctions. The solution structure of T54 I-FABP is highly homologous to that of A54 I-FABP, with the same overall three-dimensional fold that includes an antiparallel β-clam motif. Chemical shift differences between the two proteins suggest only minor local structural changes within the "portal region" and no significant alterations elsewhere. Hence, the slightly stronger binding of fatty acids to T54 I-FABP does not originate from residues in direct contact with the bound fatty acid. Instead, it appears that the larger Thr^{54} side chain affects the passage of the ligand through the entry portal. Structural details of this portal region will be discussed in view of the influence residue 54 exerts on the functional properties of human I-FABP.

The intestinal fatty acid binding protein locus (FABP2) was initially identified as a possible genetic factor determining insulin action in Pima Indians, a Native American population with a high prevalence of type 2 diabetes and obesity (*1*). A polymorphism at codon 54 of FABP2 results in an alanine-encoding allele (Ala54; frequency of 0.71) and a threonine-encoding allele (Thr54; frequency of 0.29). Pima Indians with Thr54 were more insulin resistant than Pima Indians with Ala54, as indicated by higher concentrations of plasma insulin in the fasted state, higher plasma insulin responses to both oral glucose and a mixed meal, and lower rates of insulin-stimulated glucose uptake. Furthermore, individuals with Thr54 showed higher mean fat oxidation rates (*1*). A more recent metabolic study indicated that Pima Indians homozygous for Thr54 had higher and prolonged nonesterified fatty acid responses to dietary fat, which may also contribute to insulin resistance (*2*).

Thr54 has been associated with insulin resistance also in other human populations (for a comprehensive review, see ref *3*), such as Mexican Americans (*4*), Japanese males (*5*), Korean males (*6*), and a group of Caucasians (*7*), yet showed no correlation with insulin resistance in other groups of Japanese and African American subjects (*8*−*10*). Moreover, several population-based studies suggested a role of Thr54 in alterations of the lipid metabolism. For example, Thr54 has been associated with variations in plasma triglyceride levels, lipoprotein responses, fat metabolism, and body mass in aboriginal Canadians (*11*−*13*). The Thr54 allele has further been correlated with accumulation of intra-abdominal fat in Japanese men (*5*), increased rates of fat oxidation in Korean men (*6*), higher levels of nonesterified plasma fatty

[†] This work was supported by American Heart Association Grant 9630026N to F.Z. and NIH Grants GM45859 and HL26335 to J.C.S. and J.A.H., respectively.

[‡] The ^{1}H and ^{15}N chemical shifts have been deposited in the BioMagResBank database under accession numbers 5284 (A54 I-FABP) and 5285 (T54 I-FABP). The coordinates of the human I-FABP solution structures have been deposited in the RCSB Protein Data Bank as entries 1KZW (A54) and 1KZX (T54).

* To whom correspondence should be addressed: Department of Physiology and Biophysics, Boston University School of Medicine, 715 Albany St., W302, Boston, MA 02118-2526. Phone: (617) 638-5048. Fax: (617) 638-4041. E-mail: jhamilt@bu.edu.

[§] Boston University School of Medicine.

[||] Johann Wolfgang Goethe-Universität.

[⊥] Present address: Max Planck Research Unit for Enzymology of Protein Folding, D-06120 Halle, Germany.

[@] National Institutes of Health.

[#] Texas A&M University.

10.1021/bi0273617 CCC: $25.00
Published on Web 05/30/2003

acids in obese Finns (*14*), increased postprandial lipemia (*15*), and elevated levels of fasting and postprandial plasma triglycerides in type 2 diabetic subjects (*16*). In contrast, Thr54 showed no correlation with postprandial lipid metabolism in healthy young Europeans (*17*). It has been pointed out by Weiss et al. (*3*), however, that those studies which have taken into account environmental and behavioral factors, such as individual body composition, habitual physical activity, and diet, generally deduced a connection between the Thr54 allele and insulin resistance.

Several physiological and biophysical studies have revealed altered binding and transport of long-chain fatty acids by the mutant protein. Titration microcalorimetry measurements with purified recombinant human intestinal fatty acid binding protein (I-FABP)[1] have shown that the threonine-containing (T54) protein has an ~2-fold higher affinity for oleic acid and arachidonic acid than the alanine-containing (A54) protein (*1*). Moreover, in enterocyte-mimicking cells (Caco-2 cells) that were permanently transfected to express T54 I-FABP, the apical to basolateral movement of long-chain fatty acids was faster than that in cells expressing the A54 protein (*18*). It was therefore suggested that T54 I-FABP may increase the rate of transport in the intestine and/or modulate the metabolism of dietary fatty acids by enhancing oxidation of fatty acids (*18*). In a recent study using an organ culture model for the small intestine, the A54T substitution was shown to be correlated with increased secretion of newly synthesized triglycerides and chylomicron particles (*19*). These results support the hypothesis that the polymorphism at codon 54 of FABP2 affects lipid absorption and metabolism in the small intestine.

Fatty acid binding proteins (FABPs) belong to a larger family of intracellular lipid binding proteins (*20*). Different FABPs have been isolated from a variety of tissues, including muscle, liver, myelin, adipose tissue, and the small intestine (*21*, *22*). Although their exact roles remain unclear, it is generally believed that FABPs are involved in lipid transport and trafficking (*21*, *23*). Four intracellular lipid binding proteins are expressed in the small intestine: intestinal fatty acid binding protein (I-FABP), ileal lipid binding protein (ILBP), liver fatty acid binding protein (L-FABP), and cellular retinol binding protein type II (CRBP II). The human I-FABP is a highly abundant protein expressed solely in enterocytes. It binds a single fatty acid molecule, with high affinities for both saturated and unsaturated long-chain fatty acids (*24*). The other three intestinal proteins are less specific and can bind other lipids in addition to fatty acids (*22*).

Recently, we have reported the NMR solution structures of two of the intracellular lipid binding proteins found in the intestine: human A54 I-FABP (*25*) and porcine ILBP (*26*, *27*). To help understand the molecular basis of the differences in fatty acid binding between human T54 and A54 I-FABP, we have now characterized the T54 form of human I-FABP by NMR spectroscopy. In this study, we present the sequential resonance assignment and solution structure of human T54 I-FABP and compare it to a refined structure of human A54 I-FABP.

[1] Abbreviations: FABP, fatty acid binding protein; A-FABP, adipocyte fatty acid binding protein; I-FABP, intestinal fatty acid binding protein; L-FABP, liver fatty acid binding protein; ILBP, ileal lipid binding protein; COSY, correlation spectroscopy; TOCSY, total correlation spectroscopy; NOESY, nuclear Overhauser enhancement and exchange spectroscopy; HMQC, heteronuclear multiple-quantum coherence; HSQC, heteronuclear single-quantum coherence; rmsd, root-mean-square deviation; ANS, 8-anilino-1-naphthalenesulfonic acid.

EXPERIMENTAL PROCEDURES

Materials. The pET-3d vector and BL21 cells were purchased from Novagen (Madison, WI). Isotope-labeled ammonium chloride ($^{15}NH_4Cl$, >98% ^{15}N) and sodium 3-(trimethylsilyl)[2,2,3,3-$^2H_4$]propionate were acquired from Cambridge Isotope Laboratories (Andover, MA). Isopropyl β-D-thiogalactopyranoside (IPTG) was obtained from Jersey Lab Supply (Livingston, NJ) and ammonium sulfate from ICN Pharmaceuticals (Costa Mesa, CA). Q-Sepharose and G-75 Superdex were from Pharmacia Biotech (Picataway, NJ) and the stir cell and YM3 membrane from Amicon (Beverly, MA). Deuterated water (^2H_2O, 99.9% ^2H) was purchased from Wilmad (Buena, NJ). All other chemicals that were used were analytical grade.

Expression and Purification of Human I-FABP. The human T54 I-FABP cDNA was cloned into a pET-3d vector, and the recombinant protein was expressed as described previously (*1*). Bacteria were grown either in LB medium to obtain unlabeled I-FABP or in M9 medium with $^{15}NH_4Cl$ as the sole nitrogen source to obtain ^{15}N-labeled I-FABP.

The purification procedure was performed as previously reported for A54 I-FABP (*25*). Briefly, a French press was used for bacterial lysis, followed by protamine sulfate and ammonium sulfate precipitation steps. The protein supernatant was then applied to a Q-Sepharose column, followed by G-75 Superdex column chromatography. The final concentration of purified nondelipidated T54 protein in the NMR samples was ~3 mM, in a buffer solution consisting of 20 mM KH_2PO_4, 0.05% NaN_3, and 5% ^2H_2O at pH 6.5.

NMR Experiments. A Bruker DMX 500 MHz spectrometer with a 5 mm inverse triple-resonance probe was used to carry out all NMR experiments. The NMR spectra were collected at 37 °C in a phase-sensitive mode, implementing time-proportional phase incrementation (TPPI) for quadrature detection. The ^1H and ^{15}N chemical shift values were referenced to external sodium 3-(trimethylsilyl)[2,2,3,3-$^2H_4$]propionate and 2.9 M $^{15}NH_4Cl$ in 1 M HCl, respectively. A GARP sequence (*28*) was applied during acquisition for ^{15}N decoupling. Selective presaturation was used for water suppression during the relaxation delay, with the carrier placed on the water resonance in the center of the spectrum. Presaturation was also applied during the mixing time in all NOESY experiments.

Two-dimensional (2D) NMR spectra were collected with either the ^{15}N-labeled or unlabeled protein. The time domain data size for $^1H-^1H$ total correlation spectroscopy (TOCSY) (*29*), nuclear Overhauser enhancement and exchange spectroscopy (NOESY) (*30*), $^1H-^{15}N$ 2D HMQC-TOCSY (*31*), and $^1H-^{15}N$ 2D HMQC-NOESY spectra (*32*) was 512 × 2048. The time domain data size was 1024 × 2048 for the $^1H-^1H$ double-quantum-filtered COSY (DQF-COSY) spectra (*33*) and 512 × 1024 for the $^1H-^{15}N$ heteronuclear single-quantum coherence (HSQC) spectra (*34*). After Fourier transformation, the frequency domain data size was 2048 × 2048 for the homonuclear 2D spectra and 1024 × 2048 for the heteronuclear 2D spectra. The spin-lock time for the TOCSY experiments was usually set to 80 ms. COSY-type information was obtained by running a homonuclear TOCSY

experiment with a short (3 ms) spin-lock time. A mixing time of 200 ms was used for the 2D NOESY experiments.

Three-dimensional (3D) NMR spectra were collected with the ^{15}N-labeled protein. The time domain data size for the heteronuclear 3D TOCSY-HMQC spectra (*35*, *36*) and 3D NOESY-HMQC spectra (*37*) was 256 × 64 × 1024 in the t_1 (^{1}H), t_2 (^{15}N), and t_3 (^{1}H) dimensions, respectively. These data were Fourier transformed to a 512 × 64 × 2048 matrix, and then the empty half of t_3 was discarded to obtain a final size of 512 × 64 × 1024 data points. The spin-lock time for the 3D TOCSY-HMQC experiment was set to 80 ms. A mixing time of 150 ms was used for the 3D NOESY-HMQC experiment.

The programs NMRI and TRIAD (both from Tripos, St. Louis, MO) were used for NMR data analysis. The NOE-derived distance constraints were determined from the 2D homonuclear NOESY and 3D ^{15}N-edited NOESY-HSQC spectra. Automated assignments of the NOEs, based only on chemical shifts, were obtained with the program *nmr2st* (*38*). The upper distance limits were set by an internal calibration based on the intensities of sequential and medium-range NOE values from residues within well-defined secondary structure elements. The cross-peak intensities were grouped into four different distance categories of 2.5, 3.5, 4.5, and 6.0 Å. The structure calculations were performed with the DYANA 1.5 program (*39*). Assignments of meaningful NOE cross-peaks were made by applying a structure-aided filtering strategy in repeated rounds of structure calculations. From an *ab initio* starting point, 300 conformers were calculated in 8000 annealing steps each. Stereospecific assignments of prochiral methylene and isopropyl groups were obtained using the program GLOMSA (*40*). Pseudo-atom correction for unassigned stereo partners and magnetically equivalent protons was applied as proposed by Wüthrich et al. (*41*). No hydrogen bond restraints were used in the structure calculations.

Subsequent restrained energy minimization was performed with the 20 best DYANA conformers using the DISCOVER module of the INSIGHT II program package (Accelrys, San Diego, CA). The CVFF force field (*42*) was used with a dielectric constant equal to *r* (distance in angstroms); a force constant of 20 kcal mol^{-1} Å^{-2} was applied in the NOE restraint term. The resulting structures were analyzed with PROCHECK-NMR (*43*).

RESULTS AND DISCUSSION

Structure of T54 I-FABP. The general strategy for the NMR structure determination of T54 I-FABP was essentially the same as that previously described for A54 I-FABP (*25*). Homonuclear 2D DQF-COSY, TOCSY, and NOESY as well as heteronuclear 2D HMQC-TOCSY, 2D HMQC-NOESY, 3D TOCSY-HMQC, and 3D NOESY-HMQC spectra were used for spectral assignments and subsequent structure calculations. The assignments were accomplished in two steps. The first step was to assign spin systems, where the proton resonances are grouped into different amino acid residue types via correlation-type experiments (COSY and TOCSY). The second step was to assign these spin systems sequentially by connecting them via NOE connectivities obtained from the homonuclear 2D NOESY and heteronuclear 3D NOESY-HMQC experiments. After conversion into proton distance constraints, all assigned NOE connectivities were used as input for torsion angle dynamics calculations to determine the tertiary structure of the protein.

Table 1: Structural Statistics of the 20 Selected Structures of Human T54 and A54 I-FABP after Energy Minimization

	T54	A54
structural statistics		
total no. of residues	131	131
total no. of distance restraints	2497	2538
intraresidual	211	248
sequential ($\|i-j\|=1$)	607	590
medium-range ($1<\|i-j\|\le 4$)	385	379
long-range ($\|i-j\|>4$)	1294	1321
total no. of restraint violations >0.3 Å	1	2
total no. of restraint violations >0.2 Å	15	11
maximal restraint violation (Å)	0.31	0.30
Ramachandran plot statistics (%)		
residues in most favored regions	79.7	80.4
residues in additionally allowed regions	17.8	17.1
residues in generously allowed regions	1.2	1.2
residues in disallowed regions	1.3	1.3
structural precision (Å)		
backbone atom[a] rmsd (residues 3−130)	1.09 ± 0.12	0.98 ± 0.11
heavy atom rmsd (residues 3−130)	1.68 ± 0.11	1.57 ± 0.10
backbone atom[a] rmsd (excluding portal[b])	0.97 ± 0.11	0.86 ± 0.09
backbone atom[a] rmsd (only portal[c])	1.32 ± 0.30	1.16 ± 0.28

[a] N, C$^\alpha$, C, and O. [b] Residues 3−24, 36−52, 57−71, and 77−130. [c] Residues 25−35, 53−56, and 72−76.

The ^{1}H and ^{15}N resonance assignments were completed for all amino acid residues of holo T54 I-FABP, with the exception of the N-terminal residue Ala^1. The chemical shift values of both human I-FABP forms have been deposited at the BMRB database under accession numbers 5284 (A54) and 5285 (T54). A detailed secondary structure analysis for T54 I-FABP was carried out as previously described for A54 I-FABP (*25*), where patterns of strong and weak NOE connectivities were used to identify regular secondary structure elements (data not shown). The secondary structure of T54 I-FABP is identical to that of A54 I-FABP as well as other FABPs, consisting of 10 β-strands and two short α-helices located between the first and second β-strand.

Upper distance limit constraints obtained from the NOE data were used as input for structure calculations with the program DYANA. The C$^\alpha$ traces of the 20 best conformers after restrained energy minimization are shown in Figure 1A. For a better comparison, the solution structure of the A54 protein, which had been reported previously [PDB entry 3IFB (*25*)], has now also been refined according to the new protocol (Figure 1B). The structure ensembles of holo T54 and A54 I-FABP show average backbone atom rmsd values of 1.09 ± 0.12 and 0.98 ± 0.12 Å, respectively. (Note that the positions of the fatty acid ligands have not been experimentally determined.) When superimposed (Figure 1C), both sets of conformers are highly homologous with an average backbone rmsd of 1.12 ± 0.13 Å. Overall, the protein structures are well-defined, in particular the 10 β-strands where the average rmsd values are lowest. The structural statistics of both human I-FABPs are listed in Table 1. The atomic coordinates of both I-FABP ensembles have been deposited at the RCSB Protein Data Bank as entries 1KZW (A54) and 1KZX (T54).

The three-dimensional fold of T54 I-FABP is shown schematically in Figure 2. The 10 antiparallel β-strands (A−J), which are arranged in two nearly orthogonal β-sheets, form a β-clam structure. The top of the β-clam is covered

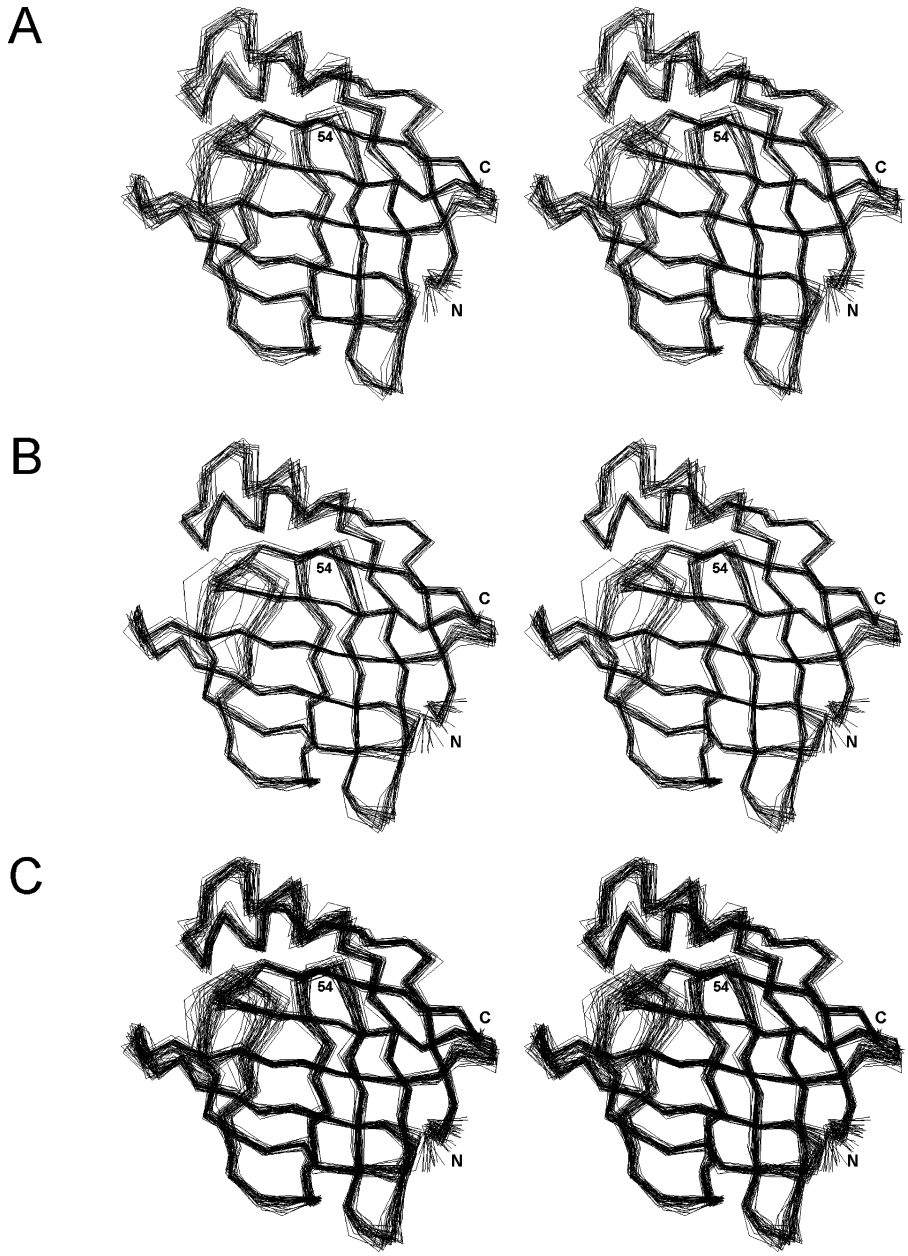

FIGURE 1: Solution structure ensembles of human T54 (A) and A54 (B) I-FABP. The C^{α} traces of the 20 best DYANA conformers after restrained energy minimization are shown superimposed in stereoplots. The average rmsd values between the backbone atoms (N, C^{α}, C, and O), excluding the terminal residues, are 1.09 ± 0.12 and 0.98 ± 0.12 Å for T54 and A54, respectively. A superposition of both ensembles (C) indicates the high degree of structural homology among all 40 conformers (average backbone atom rmsd of 1.12 ± 0.13 Å). Residue 54 and the N- and C-termini are labeled.

by two short α-helices, while a cluster of hydrophobic side chains, including Phe[2] at the N-terminus, closes the bottom of the β-clam. It has been proposed that fatty acids enter the binding cavity through an "entry portal", which is defined by the CD and EF turns as well as helix αII (*44*). In both forms of human I-FABP, this portal area (together with other β-turns and the two termini) is less well defined than the rest of the protein structure, as indicated by elevated rmsd values (see Table 1). A similar conformational variability around the portal had been previously reported also for various other intracellular lipid binding proteins (*45*). Nonetheless, the structures of the respective apo and holo forms are generally highly comparable (*46*).

Comparison between the T54 and A54 Proteins. The overall fold of T54 I-FABP is highly homologous to that of A54 I-FABP. Since chemical shift values are dependent on the electronic shielding of the surrounding atomic environment, they are very sensitive to changes in conformation and electrostatics. Hence, we compared the chemical shift values of both proteins to elucidate the effects of the A54T substitution. Heteronuclear $^{1}H-^{15}N$ HSQC spectra were used for the comparison of the amide resonances. Few significant differences were observed between the HSQC spectra of the T54 and A54 proteins, which are overlayed in Figure 3. The largest shifts, involving only residues within the portal region, are marked. All other HN resonances remain identical or nearly the same in the two I-FABP forms. This result confirms that both proteins have an almost identical structure that varies merely in the direct vicinity of the mutation site ($Ala^{54} \rightarrow Thr^{54}$).

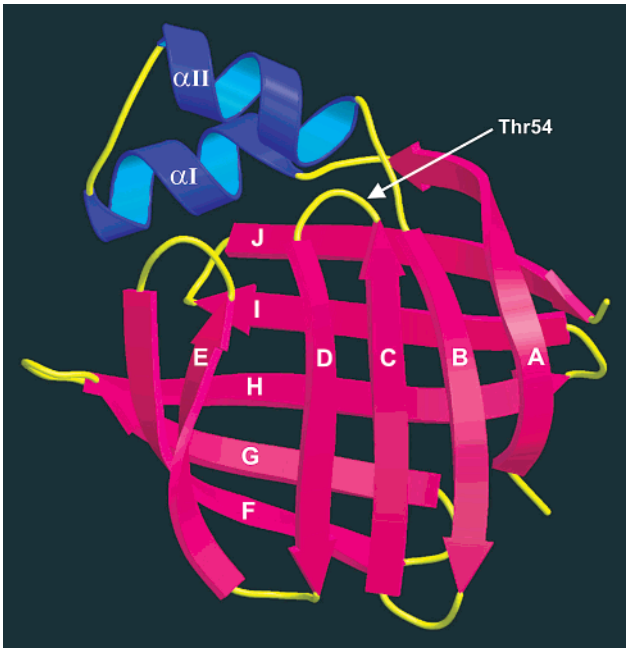

FIGURE 2: Ribbon representation of T54 I-FABP. The 10 antiparallel β-strands (A−J) and two short α-helices (αI and αII) are labeled. The fatty acid entry portal is defined by the area between helix αII and the CD β-turn, where Thr54 is located. This figure was produced with MOLSCRIPT (*67*) and Raster3D (*68*).

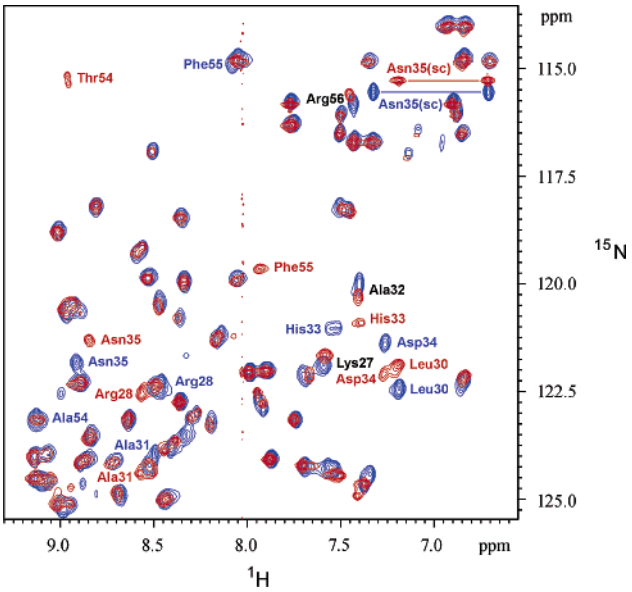

FIGURE 3: Overlay of the ^{1}H−^{15}N HSQC spectra obtained for T54 (red) and A54 (blue) I-FABP. Significant differences in chemical shift values were observed solely for residues in the portal region, as indicated in the plot with colored labels. Amide peaks of portal region residues that exhibit only minor chemical shift changes are marked with black labels.

Figure 4 shows the maximal chemical shift differences observed for each residue when comparing the backbone and side-chain proton resonances of T54 and A54 I-FABP. Clearly, the most pronounced chemical shift changes occur in residues located spatially close to the mutation site, i.e., in the CD β-turn (Ser^{53}−Arg^{56}), helix αII (Ile^{25}−His^{33}), and the subsequent αII−βB linker (Asp^{34}−Asn^{35}). The largest differences were actually found in the Leu^{30}−Asn^{35} segment as well as in Phe^{55}. In most of these cases, the maximal changes in the backbone ^{1}H resonance values pertain to the amide protons. For Asp^{34}, however, an unusually large change ($\Delta\sigma = 0.34$ ppm) of the C$^\alpha$H resonance was detected, possibly indicating a difference in its backbone conformation between T54 and A54 I-FABP. Since no such conformational differences have been observed in the two structure ensembles, an alternative explanation for this discrepancy in the Asp^{34} C$^\alpha$H chemical shift could be an alteration in the electronic shielding as a result of the more voluminous threonine side chain at position 54.

Other proton resonances that exhibited relatively large chemical shift changes include Arg^{28} HN (+0.11 ppm), Leu^{30} C$^{\delta 2}$H (+0.18 ppm), His^{33} HN (−0.21 ppm), His^{33} C$^{\epsilon 1}$H (−0.32 ppm), Asn^{35} N$^{\delta 2}$H (−0.13 ppm), and Phe^{55} HN (−0.15 ppm). Similar results were also obtained from the analysis of the backbone ^{15}N resonances, which showed significant differences between T54 and A54 I-FABP only for residues Leu^{30} (−0.6 ppm), Ala^{31} (+0.5 ppm), Asp^{34} (+0.7 ppm), Asn^{35} (+0.5 ppm), and especially Phe^{55} (+4.7 ppm). The huge effect found for the Phe^{55} nitrogen resonance is not particularly surprising, since the backbone ^{15}N chemical shift value is strongly dependent on the type of preceding residue (*47*), which in this case is the mutation site. It should be noted, however, that the side-chain NH$_2$ group of Asn^{35}, which extends toward the side chain of residue 54 in both protein forms, displays significant differences in both the ^{1}H (−0.13 ppm) and ^{15}N (−0.5 ppm) resonances, as can be seen in Figure 3. This denotes a direct influence of the A54T substitution on the Asn^{35} side chain.

Consequently, a detailed comparison of the NOE patterns between the two proteins focused on these particular residues to elucidate possible differences in their local interactions. In both human I-FABPs, residue 54 exhibits numerous NOE connectivities with residues Asp^{34} and Asn^{35}, indicating a spatial proximity as suggested by the chemical shift changes mentioned above. In addition, NOEs between the HN group of residue 54 and Leu^{36} C$^\alpha$H, between the C$^\alpha$H group of residue 54 and Arg^{56} HN, and between various protons of residue 54 and its sequential neighbors, Ser^{53} and Phe^{55}, are present in both proteins. Moreover, Phe^{55} exhibits comparable NOE connectivity patterns in both T54 and A54 I-FABP to Lys^{27}, Leu^{30}, Ala^{31}, Asp^{34}, Ser^{53}, residue 54, Arg^{56}, and Ala^{73}. Of particular interest are the side-chain to side-chain NOEs from Phe^{55} to Lys^{27} (helix αII), Leu^{30} (helix αII), and Ala^{73} (EF turn), which suggest a similar position of the phenylalanine ring in both solution structures. Nevertheless, the shift of the Leu^{30} C$^{\delta 2}$H resonance by $\Delta\sigma = +0.18$ ppm between T54 and A54 I-FABP might indicate a slightly different spatial arrangement between this side chain and the Phe^{55} phenyl ring, which is not apparent from the structure ensembles because of the high conformational dispersion in this section of the proteins.

The Phe^{55} ring, which is conserved in many FABPs, is located directly at the entrance to the binding cavity. X-ray crystallographic structures of different FABP types have displayed a variable positioning of the phenylalanine side chain at different lipidation states (*48*−*50*), which led to the hypothesis that the phenyl ring may act as an adjustable lid covering the portal (*48*). Mutagenesis studies, however, have produced divergent results regarding the effect of the Phe^{55} residue on fatty acid binding. While substitutions of the corresponding phenylalanine residues in adipocyte- and intestinal-type FABP were accompanied by weaker binding

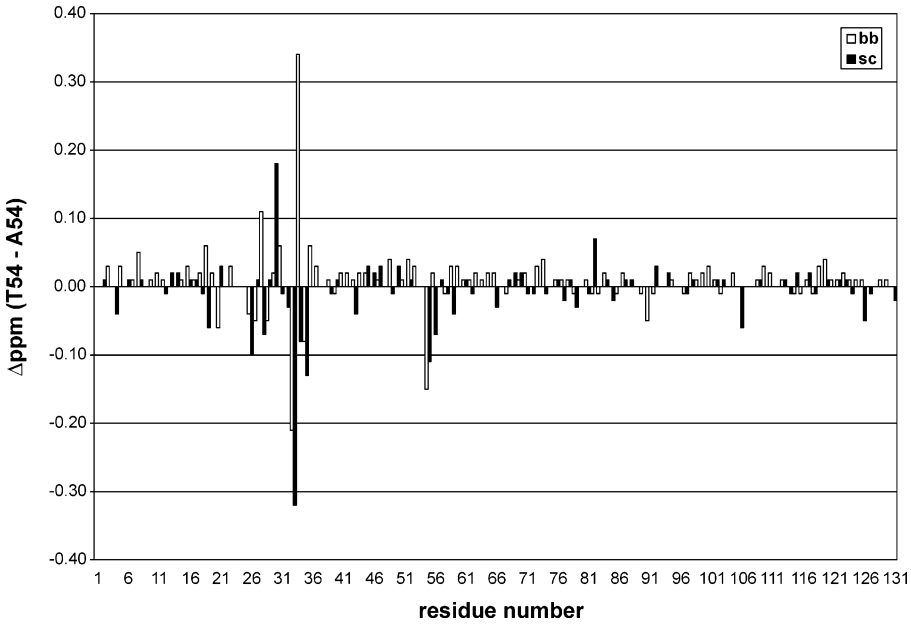

FIGURE 4: Maximal ^{1}H chemical shift changes between T54 and A54 I-FABP are indicated separately for the backbone (bb) and side-chain (sc) protons of each residue. (Note that only the largest shift difference within a residue is revealed; smaller changes, if they occur, are masked by the largest one.) The more pronounced differences in the chemical shift values occur in two distinct segments of the amino acid sequence; the largest differences are observed for residues that are spatially close to the mutation site, in particular, the Leu^{30}−Asn^{35} segment as well as Phe^{55}.

of fatty acid (*51*, *52*), a phenylalanine-to-serine mutation in human heart-type FABP had no significant effect on either binding affinity or structure compared to the wild-type protein (*53*, *54*). A recent study with a triple mutant of adipocyte-type FABP (A-FABP) that contained glycine substitutions of three portal region residues, including F57G, also showed that the fatty acid binding affinity was not markedly influenced by these steric alterations (*55*). Moreover, the closely related epidermal-type FABP lacks this particular phenylalanine residue entirely (*56*). Hence, the exact functional relevance of Phe^{55} in the various FABPs remains elusive, even though its hydrophobic interactions with neighboring portal residues as well as with the bound ligand are well-established.

The alignment of the backbone and C$^\beta$ atoms of residue 54 is basically identical in both the T54 and A54 I-FABP structures. Unfortunately, the NOE data do not sufficiently confine the additional γ-methyl and γ-hydroxyl groups of Thr^{54} to a single prevalent position. Instead, the orientation of the Thr^{54} side chain shows a rather random distribution in the 20 conformers, with the hydroxyl group pointing toward the αII−βB linker region in half of the structures, while at the same time, the methyl group extends in the opposite direction, adding to the hydrophobic character of the portal area where the Leu^{30} and Phe^{55} side chains are located (Figure 5). In this position, there are two possible scenarios in which the Thr^{54} side chain can affect ligand binding.

In the case of rat I-FABP, it has been postulated that an H-bond between the respective Asn^{54} side chain and the His^{33} C═O group stabilizes, as part of a network of capping interactions, the C-terminal part of helix αII upon ligand binding (*57*). In human I-FABP, several comparable H-bond and vdW interactions between helix αII, the CD β-turn, and the fatty acid ligand are encountered. A hydrogen bond formation is possible between Thr^{54} O$^{\gamma 1}$ and either the backbone carbonyl of His^{33} or the side-chain NH$_2$ group of Asn^{35}. Because of the high conformational variability in this particular region, and because of a lack of NOEs that would sufficiently restrain the side-chain orientation of Thr^{54}, both hydrogen bonding scenarios are found in the structure ensemble of T54 I-FABP. Our chemical shift results, however, clearly show that the A54T substitution affects most pronouncedly the residues located at the C-terminal part of

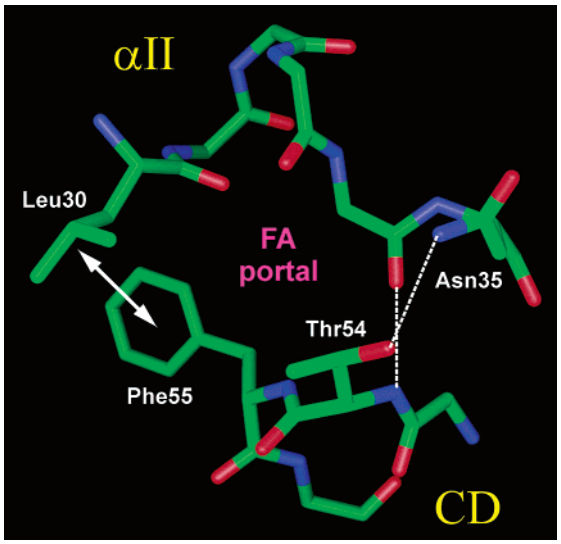

FIGURE 5: Close-up view of the portal region in T54 I-FABP. For clarity, hydrogen atoms have been omitted and side chains are displayed only for the residues that are relevant for the discussion. Shown are the intramolecular interactions that interconnect the CD β-turn and the C-terminal part of helix αII. Hydrogen bonds are represented with dashed white lines, whereas the hydrophobic vdW interaction between Leu^{30} and Phe^{55} is indicated by the white double arrow. The additional hydrogen bond between Thr^{54} O$^{\gamma 1}$ and Asn^{35} N$^{\delta 2}$H is apparently the only notable structural difference compared to A54 I-FABP. At the same time, the Thr^{54} methyl group extends toward the hydrophobic area defined by Leu^{30} and Phe^{55}. This figure was produced with GRASP (*69*).

helix αII, in particular Asp^{34} and Asn^{35}. Hence, on the basis of the chemical shift changes, the NOE patterns, the chemical polarities, and the conformer distributions, a hydrogen bond interaction between Thr^{54} and Asn^{35}, rather than His^{33}, appears to be more likely and would serve the same general purpose—to add stability to the portal region. Together with another hydrogen bridge from the HN group of residue 54 to the C═O group of Asp^{34} and the close vdW contact between the hydrophobic side chains of Leu^{30} and Phe^{55} (see Figure 5), these are the only three intramolecular interactions that interconnect the CD β-turn with the C-terminal part of helix αII. Since in the case of A54 I-FABP formation of an H-bond between the side chains of Asn^{35} and Ala^{54} is impossible, an altered conformational stability of the portal structure is likely. As previously suggested by analogy to the rat I-FABP structure (*57*), the weaker interconnection in the portal region of human A54 I-FABP could therefore be one reason why the fatty acid binding affinity is slightly lower than that of T54 I-FABP.

An alternative and even simpler explanation for the distinctions in ligand binding between A54 and T54 I-FABP, however, could be the difference in size between the alanine and threonine side chain. Previously, the portal region in rat I-FABP was studied by using a helix-less mutant protein, where the two helices were replaced with a two-residue linker (*58*, *59*). This helix-less variant had an overall structure similar to that of the wild-type protein, but it bound fatty acids with a considerably (20−100-fold) reduced affinity. Since the association rate for oleic acid was comparable to that of the wild-type protein, the lower affinity of the helix-less I-FABP appeared to be due to the dissociation rate, which was 16-fold faster for the mutant protein. More recently, a study on A-FABP focused on a triple mutant where the crucial portal region residues Val^{32}, Phe^{57}, and Lys^{58} (Leu^{30}, Phe^{55}, and Arg^{56}, respectively, in I-FABP) were replaced with glycines (*55*). As a result of this less crowded entry portal, the access rate of 8-anilino-1-naphthalene-sulfonic acid (ANS) to the binding site increased more than 500-fold. Yet the binding affinities of fatty acids and ANS changed only slightly (∼4-fold decrease for ANS), which is approximately on the same scale as the change observed for the A54T substitution in human I-FABP. The authors concluded that the size of the portal residues regulates the access to the binding site, without greatly affecting binding affinity or selectivity. Nevertheless, the absence of the vdW interaction between Val^{32} and Phe^{57} in the A-FABP mutant could play an additional role, similar to the absence of one H-bond in A54 I-FABP, by affecting the conformational stability of the portal. Hence, a combination of both the steric influence and the additional hydrogen bridge across the entry portal may be the origin of the functional differences observed between A54 and T54 I-FABP. Certainly, the access to the binding site is the key factor in both scenarios.

Kinetic binding studies with a large number of rat I-FABP mutants (*52*) have previously indicated that the k_{on} rates never significantly exceeded the wild-type value, whereas k_{off} rates varied considerably. The results for the helix-less protein (*58*) were similar, suggesting that the fatty acid binding is governed mainly by the protein−lipid interactions inside the binding site rather than by attractive forces on the protein surface. Consequently, the Thr^{54} side chain could increase the binding affinity by causing a decrease in the dissociation rate (k_{off}). We are hopeful that future experiments measuring the kinetics of fatty acid dissociation will provide further insights into the molecular mechanism that determines the difference in fatty acid binding between A54 and T54 I-FABP.

Biological Implications. Even though there are only minor local structural changes between human A54 and T54 I-FABP forms, the mutation of this single surface residue could nevertheless alter the physiological behavior of the protein. There are other examples of single-site mutations in this protein family that have a pronounced influence on the ligand binding affinity without any evident conformational changes. A glycine-to-serine mutation in the hinge region of cellular retinol binding protein rescinded ligand binding completely (*60*). In the case of heart- and adipocyte-type FABPs, the substitutions of lysines 22 and 57 also changed the binding behavior without significant structural modifications (*61*, *62*). Hence, the binding of a fatty acid can be altered by localized structural changes in a critical region.

It is furthermore possible that the A54T substitution influences other biomolecular processes that cannot be easily reproduced *in vitro*, such as interactions with cellular components (e.g., membranes or receptor molecules). Examples of such interactions have been previously reported for other intracellular lipid binding proteins. (i) Protein−membrane interactions have been proposed for several FABP types on the basis of site-directed mutagenesis studies of positively charged lysine residues located at the protein surface near the fatty acid entry portal (*63*). Modification of a single residue apparently altered the binding to model membranes and subsequently the release of ligand. (ii) The interaction of FABP with the protein-binding domain of nuclear receptors from the PPAR family, as reported for L-FABP and PPARα (*64*), which might target the fatty acid to the binding pocket of PPAR, could easily be affected by specific amino acid mutations. (iii) Finally, cellular retinoic acid binding protein type II (CRABP II) exhibits an analogous interaction with the nuclear retinoic acid receptor (RAR) to transfer retinoic acid (*65*). Even though its closest relative (74% sequence identity), cellular retinoic acid binding protein type I (CRABP I), has the same tertiary structure and only a 2-fold higher ligand binding affinity (*66*), it does not deliver retinoic acid to the receptor. The substitution of three surface residues near the entry portal, however, enables CRABP I to mimic the biological activity of CRABP II.

In T54 I-FABP, the larger side chain of residue 54 may in part block the entry portal and/or alter its conformational stability by a single additional hydrogen bond across the portal, subsequently causing the bound ligand to remain locked inside the protein cavity for a longer period of time. With all other factors remaining constant, this could account for the higher affinity of long-chain fatty acids for the T54 protein than for the wild type, but does not yet explain the physiological differences observed in individuals who carry the Thr54 allele.

REFERENCES

1. Baier, L. J., Sacchettini, J. C., Knowler, W. C., Eads, J., Paolisso, G., Tataranni, P. A., Mochizuki, H., Bennett, P. H., Bogardus, C., and Prochazka, M. (1995) An amino acid substitution in the

human intestinal fatty acid binding protein is associated with increased fatty acid binding, increased fat oxidation, and insulin resistance, *J. Clin. Invest. 95*, 1281−1287.
2. Pratley, R. E., Baier, L., Pan, D. A., Salbe, A. D., Storlien, L., Ravussin, E., and Bogardus, C. (2000) Effects of an Ala54Thr polymorphism in the intestinal fatty acid-binding protein on responses to dietary fat in humans, *J. Lipid Res. 41*, 2002−2008.
3. Weiss, E. P., Brown, M. D., Shuldiner, A. R., and Hagberg, J. M. (2002) Fatty acid binding protein-2 gene variants and insulin resistance: gene and gene-environment interaction effects, *Physiol. Genomics 10*, 145−157.
4. Mitchell, B. D., Kammerer, C. M., O'Connell, P., Harrison, C. R., Manire, M., Shipman, P., Moyer, M. P., Stern, M. P., and Frazier, M. C. (1995) Evidence for linkage of postchallenge insulin levels with intestinal fatty acid-binding protein (FABP2) in Mexican-Americans, *Diabetes 44*, 1046−1053.
5. Yamada, K., Yuan, X., Ishiyama, S., Koyama, K., Ichikawa, F., Koyanagi, A., Koyama, W., and Nonaka, K. (1997) Association between Ala54Thr substitution of the fatty acid-binding protein 2 gene with insulin resistance and intra-abdominal fat thickness in Japanese men, *Diabetologica 40*, 706−710.
6. Kim, C.-H., Yun, S.-K., Byun, D.-W., Yoo, M.-H., Lee, K.-U., and Suh, K. I. (2001) Codon 54 polymorphism of the fatty acid binding protein 2 gene is associated with increased fat oxidation and hyperinsulinemia, but not with intestinal fatty acid absorption in Korean men, *Metabolism 50*, 473−476.
7. Chiu, K. C., Chuang, L.-M., Chu, A., and Yoon, C. (2001) Fatty acid binding protein 2 and insulin resistance, *Eur. J. Clin. Invest. 31*, 521−527.
8. Hayakawa, T., Nagai, Y., Nohara, E., Yamashita, H., Takamura, T., Abe, T., Nomura, G., and Kobayashi, K.-i. (1999) Variation of the fatty acid binding protein 2 gene is not associated with obesity and insulin resistance in Japanese subjects, *Metabolism 48*, 655−657.
9. Ito, K., Nakatani, K., Fujii, M., Katsuki, A., Tsuchihashi, K., Murata, K., Goto, H., Yano, Y., Gabazza, E. C., Sumida, Y., and Adachi, Y. (1999) Codon 54 polymorphism of the fatty acid binding protein gene and insulin resistance in the Japanese population, *Diabetes Med. 16*, 119−124.
10. Lei, H.-H., Coresh, J., Shuldiner, A. R., Boerwinkle, E., and Brancati, F. L. (1999) Variants of the insulin receptor substrate-1 and fatty acid binding protein 2 genes and the risk of type 2 diabetes, obesity, and hyperinsulinemia in African-Americans: the Atherosclerosis Risk in Communities Study, *Diabetes 48*, 1868−1872.
11. Hegele, R. A., Harris, S. B., Hanley, A. J. G., Sadikian, S., Connelly, P. W., and Zinman, B. (1996) Genetic variation of intestinal fatty acid-binding protein associated with variation in body mass in aboriginal Canadians, *J. Clin. Endocrinol. Metab. 81*, 4334−4337.
12. Hegele, R. A., Wolever, T. M. S., Story, J. A., Connelly, P. W., and Jenkins, D. J. A. (1997) Intestinal fatty acid-binding protein variation associated with variation in the response of plasma lipoproteins to dietary fibre, *Eur. J. Clin. Invest. 27*, 857−862.
13. Hegele, R. A., Connelly, P. W., Hanley, A. J. G., Sun, F., Harris, S. B., and Zinman, B. (1997) Common genomic variants associated with variation in plasma lipoproteins in young aboriginal Canadians, *Arterioscler., Thromb., Vasc. Biol. 17*, 1060−1066.
14. Vidgren, H. M., Sipiläinen, R. H., Heikkinen, S., Laakso, M., and Uusitupa, M. I. J. (1997) Threonine allele in codon 54 of the fatty acid binding protein 2 gene does not modify the fatty acid composition of serum lipids in obese subjects, *Eur. J. Clin. Invest. 27*, 405−408.
15. Ågren, J. J., Valve, R., Vidgren, H., Laakso, M., and Uusitupa, M. (1998) Postprandial lipemic response is modified by the polymorphism at codon 54 of the fatty acid-binding protein 2 gene, *Arterioscler., Thromb., Vasc. Biol. 18*, 1606−1610.
16. Georgopoulos, A., Aras, O., and Tsai, M. Y. (2000) Codon-54 polymorphism of the fatty acid-binding protein 2 gene is associated with elevation of fasting and postprandial triglyceride in type 2 diabetes, *J. Clin. Endocrinol. Metab. 85*, 3155−3160.
17. Tahvanainen, E., Molin, M., Vainio, S., Tiret, L., Nicaud, V., Farinaro, E., Masana, L., and Ehnholm, C. (2000) Intestinal fatty acid binding protein polymorphism at codon 54 is not associated with postprandial responses to fat and glucose tolerance tests in healthy young Europeans. Results from EARS II participants, *Atherosclerosis 152*, 317−325.
18. Baier, L. J., Bogardus, C., and Sacchettini, J. C. (1996) A polymorphism in the human intestinal fatty acid binding protein alters fatty acid transport across Caco-2 cells, *J. Biol. Chem. 271*, 10892−10896.
19. Levy, E., Ménard, D., Delvin, E., Stan, S., Mitchell, G., Lambert, M., Ziv, E., Feoli-Fonseca, J. C., and Seidman, E. (2001) The polymorphism at codon 54 of the FABP2 gene increases fat absorption in human intestinal explants, *J. Biol. Chem. 276*, 39679−39684.
20. Banaszak, L. B., Winter, N., Xu, Z., Bernlohr, D. A., Cowan, S., and Jones, T. A. (1994) Lipid-binding proteins: a family of fatty acid and retinoid transport proteins, *Adv. Protein Chem. 45*, 89−151.
21. Veerkamp, J. H., Peeters, R. A., and Maatman, R. G. H. J (1991) Structural and functional features of different types of cytoplasmic fatty acid-binding proteins, *Biochim. Biophys. Acta 1081*, 1−24.
22. Veerkamp, J. H., and Maatman, R. G. H. J (1995) Cytoplasmic fatty acid-binding proteins: their structure and genes, *Prog. Lipid Res. 34*, 17−52.
23. Kaikaus, R. M., Bass, N. M., and Ockner, R. K. (1990) Functions of fatty acid binding proteins, *Experientia 46*, 617−630.
24. Lowe, J. B., Sacchettini, J. C., Laposata, M., McQuillan, J. J., and Gordon, J. I. (1987) Expression of rat intestinal fatty acid-binding protein in *Escherichia coli*. Purification and comparison of ligand binding characteristics with that of *Escherichia coli*-derived rat liver fatty acid-binding protein, *J. Biol. Chem. 262*, 5931−5937.
25. Zhang, F., Lücke, C., Baier, L. J., Sacchettini, J. C., and Hamilton, J. A. (1997) Solution structure of human intestinal fatty acid binding protein: implications for ligand entry and exit, *J. Biomol. NMR 9*, 213−228.
26. Lücke, C., Zhang, F., Rüterjans, H., Hamilton, J. A., and Sacchettini, J. C. (1996) Flexibility is a likely determinant of binding specificity in the case of ileal lipid-binding protein, *Structure 4*, 785−800.
27. Lücke, C., Zhang, F., Hamilton, J. A., Sacchettini, J. C., and Rüterjans, H. (2000) Solution structure of ileal lipid binding protein in complex with glycocholate, *Eur. J. Biochem. 267*, 2929−2938.
28. Shaka, A. J., Barker, P. B., and Freeman, R. (1985) Computer-optimized decoupling scheme for wideband applications and low-level operation, *J. Magn. Reson. 64*, 547−552.
29. Griesinger, C., Otting, G., Wüthrich, K., and Ernst, R. R. (1988) Clean-TOCSY for ^{1}H spin system identification in macromolecules, *J. Am. Chem. Soc. 110*, 7870−7872.
30. Jeener, J., Meier, B. H., Bachmann, P., and Ernst, R. R. (1979) Investigation of exchange processes by two-dimensional NMR spectroscopy, *J. Chem. Phys. 71*, 4546−4553.
31. Lerner, L., and Bax, A. (1986) Sensitivity-enhanced two-dimensional heteronuclear relayed coherence transfer NMR spectroscopy, *J. Magn. Reson. 69*, 375−380.
32. Shon, K., and Opella, S. J. (1989) Detection of ^{1}H homonuclear NOE between amide sites in proteins with ^{1}H/^{15}N heteronuclear correlation spectroscopy, *J. Magn. Reson. 71*, 379−383.
33. Piantini, U., Sørensen, O. W., and Ernst, R. R. (1980) Multiple quantum filters for elucidating NMR coupling networks, *J. Am. Chem. Soc. 104*, 6800−6801.
34. Bodenhausen, G., and Ruben, D. J. (1980) Natural abundance nitrogen-15 NMR by enhanced heteronuclear spectroscopy, *Chem. Phys. Lett. 69*, 185−191.
35. Marion, D., Kay, L. E., Sparks, S. W., Torchia, D. A., and Bax, A. (1989) Three-dimensional heteronuclear NMR of ^{15}N-labeled proteins, *J. Am. Chem. Soc. 111*, 1515−1517.
36. Zuiderweg, E. P. R., and Fesik, S. W. (1989) Heteronuclear three-dimensional NMR spectroscopy of the inflamatory protein C5a, *Biochemistry 28*, 2387−2391.
37. Marion, D., Driscoll, P. C., Kay, L. E., Wingfield, P. T., Bax, A., Gronenborn, A. M., and Clore, G. M. (1989) Overcoming the overlap problem in the assignment of ^{1}H NMR spectra of larger proteins by use of three-dimensional heteronuclear ^{1}H-^{15}N Hartmann−Hahn-multiple quantum coherence and nuclear Overhauser-multiple quantum coherence spectroscopy: application to interleukin 1β, *Biochemistry 28*, 6150−6156.
38. Pristovšek, P., Lücke, C., Reincke, B., Ludwig, B., and Rüterjans, H. (2000) Solution structure of the functional domain of *Paracoccus denitrificans* cytochrome c_{552} in the reduced state, *Eur. J. Biochem. 267*, 4205−4212.
39. Güntert, P., Mumenthaler, C., and Wüthrich, K. (1997) Torsion angle dynamics for NMR structure calculation with the new program DYANA, *J. Mol. Biol. 273*, 283−298.

40. Güntert, P., Braun, W., and Wüthrich, K. (1991) Efficient computation of three-dimensional protein structures in solution from nuclear magnetic resonance data using the program DIANA and the supporting programs CALIBA, HABAS and GLOMSA, *J. Mol. Biol. 217*, 517−530.
41. Wüthrich, K., Billeter, M., and Braun, W. (1983) Pseudo-structures for the 20 common amino acids for use in studies of protein conformations by measurements of intramolecular proton−proton distance constraints with nuclear magnetic resonance, *J. Mol. Biol. 169*, 949−961.
42. Dauber-Osguthorpe, P., Roberts, V. A., Osguthorpe, D. J., Wolff, D. J., Genest, M., and Hagler, A. T. (1988) Structure and energetics of ligand binding to proteins: *E. coli* dihydrofolate reductase trimethoprin, a drug-receptor system, *Proteins 4*, 31−47.
43. Laskowski, R. A., Rullmann, J. A. C., MacArthur, M. W., Kaptein, R., and Thornton, J. M. (1996) AQUA and PROCHECK-NMR: programs for checking the quality of protein structures solved by NMR, *J. Biomol. NMR 8*, 477−486.
44. Sacchettini, J. C., Scapin, G., Gopaul, D., and Gordon, J. I. (1992) Refinement of the structure of *Escherichia coli*-derived rat intestinal fatty acid binding protein with bound oleate to 1.75-Å resolution, *J. Biol. Chem. 267*, 23534−23545.
45. Hanhoff, T., Lücke, C., and Spener, F. (2002) Insights into binding of fatty acids by fatty acid binding proteins, *Mol. Cell. Biochem. 239*, 45−54.
46. Lücke, C., Gutiérrez-González, L. H., and Hamilton, J. A. (2003) Intracellular lipid binding proteins: evolution, structure and ligand binding, in *Cellular Proteins and Their Fatty Acids in Health and Disease* (Duttaroy, A. K., and Spener, F., Eds.) pp 95−118, Wiley-VCH, Weinheim, Germany.
47. de Dios, A. C., Pearson, J. G., and Oldfield, E. (1993) Secondary and tertiary structural effects on protein NMR chemical shifts: an ab initio approach, *Science 260*, 1491−1496.
48. Eads, J., Sacchettini, J. C., Kromminga, A., and Gordon, J. I. (1993) *Escherichia coli*-derived rat intestinal fatty acid binding protein with bound myristate at 1.5 Å resolution and I-FABP (R106Q) with bound oleate at 1.74 Å resolution, *J. Biol. Chem. 268*, 26375−26385.
49. Xu, Z., Bernlohr, D. A., and Banaszak, L. J. (1993) The adipocyte lipid-binding protein at 1.6 Å resolution, *J. Biol. Chem. 268*, 7874−7884.
50. Young, A. C. M., Scapin, G., Kromminga, A., Patel, S. B., Veerkamp, J. H., and Sacchettini, J. C. (1994) Structural studies on human muscle fatty acid binding protein at 1.4 Å resolution: binding interactions with three C18 fatty acids, *Structure 2*, 523−534.
51. Simpson, M. A., and Bernlohr, D. A. (1998) Analysis of a series of phenylalanine 57 mutants of the adipocyte lipid-binding protein, *Biochemistry 37*, 10980−10986.
52. Richieri, G. V., Low, P. J., Ogata, R. T., and Kleinfeld, A. M. (1999) Binding kinetics of engineered mutants provide insight about the pathway for entering and exiting the intestinal fatty acid binding protein, *Biochemistry 38*, 5888−5895.
53. Prinsen, C. F. M., and Veerkamp, J. H. (1996) Fatty acid binding and conformational stability of mutants of human muscle fatty acid-binding protein, *Biochem. J. 314*, 253−260.
54. Lücke, C., Rademacher, M., Zimmerman, A. W., van Moerkerk, H. T. B., Veerkamp, J. H., and Rüterjans, H. (2001) Spin-system heterogeneities indicate a selected-fit mechanism in fatty acid binding to heart-type fatty acid-binding protein (H-FABP), *Biochem. J. 354*, 259−266.
55. Jenkins, A. E., Hockenberry, J. A., Nguyen, T., and Bernlohr, D. A. (2002) Testing of the portal hypothesis: analysis of a V32G, F57G, K58G mutant of the fatty acid binding protein of the murine adipocyte, *Biochemistry 41*, 2022−2027.
56. Hohoff, C., Börchers, T., Rüstow, B., Spener, F., and van Tilbeurgh, H. (1999) Expression, purification and crystal structure determination of recombinant human epidermal-type fatty acid binding protein, *Biochemistry 38*, 12229−12239.
57. Hodsdon, M. E., and Cistola, D. P. (1997) Discrete backbone disorder in the nuclear magnetic resonance structure of apo intestinal fatty acid-binding protein: Implications for the mechanism of ligand entry, *Biochemistry 36*, 1450−1460.
58. Cistola, D. P., Kim, K., Rogl, H., and Frieden, C. (1996) Fatty acid interactions with a helix-less variant of intestinal fatty acid-binding protein, *Biochemistry 35*, 7559−7565.
59. Kim, K., Cistola, D. P., and Frieden, C. (1996) Intestinal fatty acid-binding protein: the structure and stability of a helix-less variant, *Biochemistry 35*, 7553−7558.
60. van Aalten, D. M. F., Jones, P. C., de Sousa, M., and Findlay, J. B. C. (1997) Engineering protein mechanics: inhibition of concerted motions of the cellular retinol binding protein by site-directed mutagenesis, *Protein Eng. 10*, 31−37.
61. Herr, F. M., Aronson, J., and Storch, J. (1996) Role of portal region lysine residues in electrostatic interactions between heart fatty acid binding protein and phospholipid membranes, *Biochemistry 35*, 1296−1303.
62. Liou, H. L., and Storch, J. (2001) Role of surface lysine residues of adipocyte fatty acid-binding protein in fatty acid transfer to phospholipid vesicles, *Biochemistry 40*, 6475−6485.
63. Storch, J., Herr, F. M., Hsu, K. T., Kim, H. K., Liou, H. L., and Smith, E. R. (1996) The role of membranes and intracellular binding proteins in cytoplasmic transport of hydrophobic molecules: fatty acid-binding proteins, *Comp. Biochem. Physiol., Part B: Biochem. Mol. Biol. 115*, 333−339.
64. Wolfrum, C., Borrmann, C. M., Börchers, T., and Spener, F. (2001) Fatty acids and hypolipidemic drugs regulate peroxisome proliferator-activated receptors α- and γ-mediated gene expression via liver fatty acid-binding protein: a signalling path to the nucleus, *Proc. Natl. Acad. Sci. U.S.A. 98*, 2323−2328.
65. Budhu, A., Gillilan, R., and Noy, N. (2001) Localization of the RAR interaction domain of cellular retinoic acid binding protein-II, *J. Mol. Biol. 305*, 939−949.
66. Dong, D., Ruuska, S. E., Levinthal, D. J., and Noy, N. (1999) Distinct roles for cellular retinoic acid-binding proteins I and II in regulating signaling by retinoic acid, *J. Biol. Chem. 274*, 23695−23698.
67. Kraulis, P. J. (1991) MOLSCRIPT: a program to produce both detailed and schematic plots of protein structures, *J. Appl. Crystallogr. 24*, 946−950.
68. Merritt, E. A., and Bacon, D. J. (1997) Raster3D: photorealistic molecular graphics, *Methods Enzymol. 277*, 505−524.
69. Nicholls, A., Sharp, K. A., and Honig, B. (1991) Protein folding and association: Insights from the interfacial and thermodynamic properties of hydrocarbons, *Proteins 11*, 281−296.

BI0273617